Preprint

This is the submitted version of a paper published in *Sensors and actuators. B, Chemical*.

Permanent link to this version:
http://urn.kb.se/resolve?urn=urn:nbn:se:uu:diva-210959

Controllable growth of ZnO nanowires grown on discrete islands of Au catalyst for realization of planar-type micro gas sensors

Hugo Nguyen[1,*], Chu Thi Quy[2,3], Nguyen Duc Hoa[2], Nguyen The Lam[3],

Nguyen Van Duy[2], Vu Van Quang[2], Nguyen Van Hieu[2,*]

[1] Department of Engineering Sciences, Division of Microsystem Technology, Uppsala University, Sweden

[2] International Training Institute for Materials Science (ITIMS), Hanoi University of Science and Technology, Hanoi, Viet Nam

[3] Faculty of Physics, Hanoi Pedagogical University No 2, Vinhphuc, Viet Nam

Corresponding authors
*Hugo Nguyen, Associate Professor
Department of Engineering Sciences, Division of Microsystem Technology,
Uppsala University, Sweden
Address:
Tel: +46 184716838 ; Fax: +46 184713572
Email: hugo.nguyen@angstrom.uu.se

*Nguyen Van Hieu, *Associate Professor*
International Training Institute for Materials Science (ITIMS),
Hanoi University of Science and Technology (HUST)
Address: No.1, Dai Co Viet Str., Hanoi, Vietnam
Tel: 84 4 38680787;   Fax: 84 4 38692963
Email: hieu@itims.edu.vn

Abstract: The proper engineering design of gas sensors and the controlled synthesis of sensing materials for the high-performance detection of toxic gas are very important in the fabrication of handheld devices. In this study, an effective design for gas sensor chips is developed to control the formation of grown ZnO nanowires (NWs). The design utilizes the dendrite islands of Au catalyst deposited on and between Pt electrodes of a planar-type micro gas sensor so that NWs can grow on instead of a continuous Au seed layer. This method results in an increase of NW-NW junctions on the device and also eliminates current leakage through the seed layer, which results in a higher sensitivity. The results show that the developed gas-sensing devices could be used to monitor NO_2 at moderate temperature (~250 °C) and/or ethanol at a high temperature (~400 °C).

Keywords: ZnO nanowires, on-chip growth, MEMS, planar-type sensors

1. Introduction

The increase in air pollution from toxic and flammable gases, such as NO_2, CO, NH_3, H_2S, and volatile organic compounds (VOCs), is one of the critical factors that cause global warming, climate change, and human illnesses [1]. Attempts to develop compact, small size, low-cost, low-power consumption, and high-performance gas sensors for the early and accurate detection and/or monitoring of these gases have been carried out not only to protect humans from being exposed to hazardous agents but also to help improve the living environment and prevent environmental disasters [2].

The use of resistive-type ZnO nanorods (NRs) and NWs as materials for gas sensing has been intensively studied because of their excellent chemical-thermal stability and relatively high sensitivity to different gases [3][4]. Various techniques have been developed for the fabrication

of nanostructued ZnO, the most common of which is hydrothermal synthesis because of its easy scaling up of production and easy control of the length and the diameter of NWs [5], [6]. However, recently reported experiments are limited to the fabrication of and investigation on the gas-sensing properties of ZnO NRs/NWs and have not investigated the design and fabrication of compacted devices [7]: Shinde reported on the synthesis of ZnO NRs via spray pyrolysis for H_2S gas sensor [8]; Hu et al. reported on the highly formaldehyde-sensitive, transition-metal doped ZnO NRs prepared via plasma-enhanced chemical vapor deposition [9]; and Rai et al. reported on the microwave-assisted hydrothermal synthesis of ZnO NRs for gas sensor application [10].

For the practical use of gas sensors, proper designs and fabrication processes of compacted devices that offer low power consumption and low production cost are expected to open new markets for handheld devices [11]. The MEMS technique has been employed for the fabrication of thin films [13] and nanodots [14] to fabricate gas sensing materials. Moon et al. reported on a low power consumption NO_2 micro gas sensor based on semiconducting SnO_2 nano-powders synthesized via a co-precipitation method. They designed and fabricated a micro-heater by using MEMS processes and the screen-printing technique [15]. Pandya et al. fabricated an ethanol sensor, where ZnO nanoflakes were grown by annealing an evaporated thin film of Zn at a high temperature [16]. Ting et al. demonstrated the lateral growth of ZnO NWs on chips via self-catalyzed reactive thermal evaporation, and the product can be used for ethanol detection [17], where the number of NWs that bridge the electrodes to one another was increased to enhance the sensitivity of sensors. The on-chip grown semiconducting metal oxide NRs/NWs for gas sensor applications was believed to have significant advantages in both fabrication process and sensor performance [18], [19]. However, other ways to apply the sensing material on chips are available. For instance, in the study by Guo et al., ZnO NWs were first grown via hydrothermal

method, dispersed into an ethanol solution, and dropped onto pre-deposited electrodes [20]. Dielectrophoretic post synthesis was performed to align the ZnO NWs across the interdigitated electrodes to produce a sensor capable of UV detection. The hydrothermal synthesis of vertical ZnO NRs via a well-known hexamethyltetramine route requires the use of a ZnO seed layer [21], [22], whereas the conventional CVD method requires assistance from a noble metal catalytic layer [23]. The on-chip growth of ZnO NRs/NWs also requires a kind of seed or catalyst layer on any surface. Unfortunately, this process leads to the risk of current leakage through the seed or catalyst layer when sensing, which results in a decrease in sensitivity [24]. However, the possibility of controlling the length and density of NWs, and thus the number of NW-NW junctions that form directly on the chips, may influence gas sensor performance because a higher number of NW-NW junctions is expected to enhance the gas sensing properties of the sensors.

Herein, we introduce an effective design for the on-chip growth of ZnO NWs to control the length and density of the wires to fabricate highly sensitive gas sensors. The design utilizes the dendrite islands of an Au catalyst deposited on and between the electrodes for the growth of NWs. The use of dendrite catalyst islands instead of an ordinary continuous thin film of a seed/catalyst material leads to (i) an increase in the number of NW-NW junctions on the devices and (ii) the prevention of current leakage through the ordinary seed layer, which results in a higher sensitivity. The MEMS technology was also used to downsize the sensing devices to reduce the power consumption.

2. Experimental

The design and the MEMS processes used for the fabrication of the sensor chips are illustrated in Figure 1(A) and (B), respectively. The sensor design is composed of a microheater and a pair of

electrodes made up of Pt/Cr deposited on a SiN coated silicon membrane, as seen in Figure 1(Aa). The NW-NW junctions function as electric conducting paths for the sensing measurement, as seen in Figure 1(Ab). The MEMS processes for the fabrication of the sensor chips involve the deposition of Pt/Cr electrode and heaters, the deposition of dendrite Au islands as catalyst, and the back side dry etching of Si to reduce the power consumption of the devices. The detailed processes, as seen in Figure 1(B), can be summarized as follows: after cleaning in acetone, IPA, water rinsing and spinning to dry, the silicon wafer was covered with 300 nm SiN and underwent the ordinary UV-lithography steps (1 μm thick photoresist 1813, soft baked at 115 °C for 1 min, exposed for 6 s, hard contact, gap 40 μm, and developed for 1 min). A mask was used in these steps for pattern heaters and electrodes for chips of 4x4 mm, as seen in Figure 1(Ba). After vapor deposition of 10 nm Cr and 200 nm Pt (Evaporator-Lesker TMP, PVD75), lift-off was done in acetone and assisted by ultrasonic vibration, as illustrated in Figure 1(Bb) and (Bc). The wafer was then rinsed with water, spun to dry, and once again underwent the lithography and lift-off steps similar to the steps described above, except that another mask was used and 10 nm Au was sputtered to create Au islands between and on the electrodes for catalytic purpose in later NW growth, as can be seen in Figure 1(Bd) and (Be). Back side dry etching of Si was performed for 40 minutes (110 S/DE, Tegal Corporation, USA) to a depth of 475 microns to obtain a membrane of about 50 microns, as illustrated in Figure 1(Bf). The wafer was then diced into sensor chips of 4x4 mm for ZnO NWs growth, as illustrated in Figure 1(Bh).
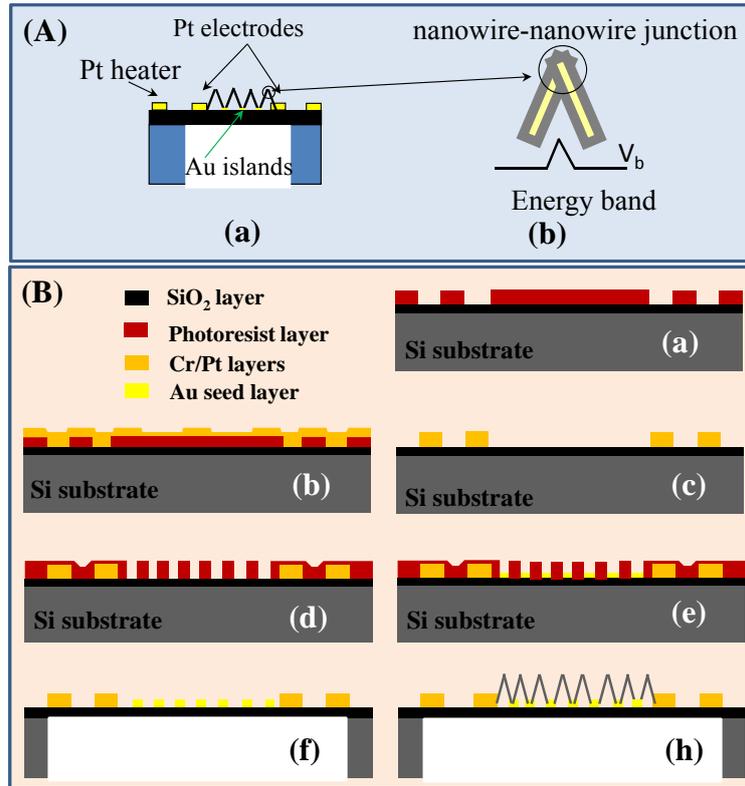
Figure 1. (A) ZnO NW-based sensors: (a) design of the sensor, (b) NW-NW junction model; and (B) Experimental procedures to fabricate the sensors; (a) deposition and patterning of the photoresist layer, (b) deposition of Cr/Pt layers, (c) lift-off to pattern the Cr/Pt electrodes, (d) deposition and patterning of the photoresist layer, (e) deposition of the Au catalytic layer, (f) lift-off to pattern the Au catalytic islands, and dry etching the back side silicon, and (h) growth of ZnO nanowires.

ZnO NWs were synthesized on the sensor chips via the carbothermal route by using a mixture of ZnO powder and carbon (50% wt.) as source materials [25]. In a typical synthesis, 0.1 gram of source material is loaded in an alumina boat and placed in center of a quartz tube furnace. Thereafter, a silicon substrate composed of 20 chips is introduced into center of the quartz tube furnace, 3 cm away from the alumina boat. Before the growth process started, the

quartz tube was pumped down to a pressure of 2×10^{-2} torr, and high purity argon gas was introduced to the tube for an hour to clean out the residual oxygen. During the NW growth, the pressure inside the quartz tube was maintained at 1.5×10^{-1} torr by flowing a mixture of argon and oxygen at a rate of 30 and 5 sccm, respectively. The temperature of the furnace was then rapidly increased to a growth temperature of 950 °C within 30 min and maintained at this temperature for ZnO NW growth. To control the length and density of the ZnO NWs, the growth time was varied (and kept for 10, 20, 40, and 60 min for four different growth experiments). Finally, the quartz tube furnace was naturally cooled down to room temperature.

The morphology and size distribution of NWs were characterized via field emission scanning electron microscopy (FE-SEM) (Hitachi S4800 operated at 15 keV) and transmission electron microscopy (TEM) (JEOL, Model 2100F). Material crystallography was verified via X-ray diffraction (XRD) analysis. The optical properties of the NWs were studied using room temperature-photoluminescence (PL) measurement and Raman spectroscopy.

The gas sensors were tested via a flow-through technique with a standard flow rate of 400 sccm for both dry air and balanced gas by using an in-house sensing system developed by iSensors group (www.iSensors.vn). This sensing system enabled rapid switching (~1 s) from dry air to analytic gas. In the experiment, the standard gas of a mixture of NO_2, H_2, and ethanol at concentrations of 1,000, 10,000, and 10,000 ppm, respectively, were used. The standard gas was mixed with dry air as carrier by using a series of mass flow controllers to obtain a lower concentration. By varying the flow rate ratio of the standard gas and dry air, different concentrations of the test gas were obtained. The gas concentrations were calculated as $C(ppm)=C_{std}(ppm) \times f/(f+F)$, where f, and F are the flow rate of the analytic gas and dry air, respectively. $C_{std}(ppm)$ is the concentration of the standard gas used in the experiment. Before

the measurements were taken, dry air was flown through the sensing chamber until the sensor resistance stabilized. During the sensing measurement, the resistance of the sensors was continuously measured using a Keithley (model 2700) interfaced with a computer, whereas dry air and the analytic gases were switched on/off each cycle. The sensor response was defined as $S(\%) = 100 \times (R_{NO2}-R_{air})/R_{air}$ for oxidizing gas (NO_2) and $S(\%) = 100 \times (R_{air}-R_{gas})/R_{gas}$ for reducing gases such as H_2 and EtOH, where R_{gas}, $R_{NO2,}$ and R_{air} are the sensor resistances in the presence of reducing gases, NO_2, and dry air, respectively.

3. Results and discussion

The dependence of the sensor chip temperature on the applied power measured using an infrared thermography (IR camera A40, FLIR Systems, USA) is shown in Figure 2. As demonstrated, the chip temperature increased linearly with the applied power, and in this case, the temperature was varied from room temperature to 500 °C, Figure 2(A). This temperature covers a wide range because the sensing measurement usually requires a working temperature of about 200 °C to 450 °C [13]. The temperature distribution of the sensor chip investigated via infrared thermography, shown in Figure 2(B), demonstrated that the heat is concentrated at the center of the chip because of its MEMS structure, wherein the back side silicon was etched down to create the membrane; thus, heat dissipation and power consumption are reduced. The miniaturization of the sensing devices also reduced the thermal time constants because the small area and low mass of the active sensor membrane allows faster temperature cycling [26].
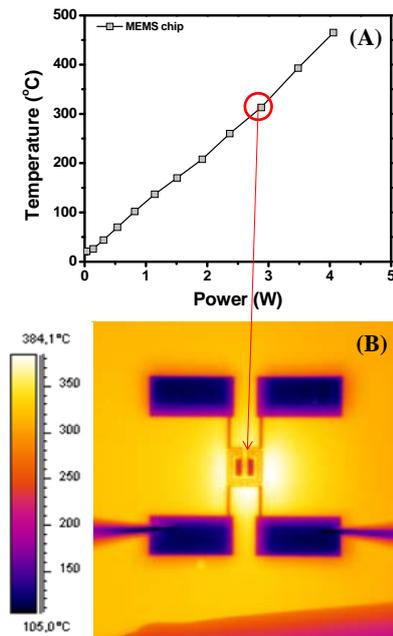
Figure 2. *(A) Temperature dependence of the MEMS-chip on the applied power; (B) infrared thermography image of the MEMS-chip at an operating temperature of 350 °C.*

Controlling the length of the ZnO NWs that grow on the pre-defined MEMS chips is very important to ensure that the devices work properly. If the ZnO wires are too short, they cannot make any NW-NW junction. If they are too long (and if they start to grow outside the Au islands) current leakage or even short-circuiting of the Pt electrodes and micro-heater may occur. In this study, the growth time was varied from 10, 20, 40, and 60 min while all others parameters, such as growth temperature (950 °C), gas flowing rate, growth pressure, and initial weight of source material, were fixed. Figure 3(A-D) shows the FE-SEM images of the ZnO NWs grown for 10, 20, 40, and 60 min, respectively, on the sensor chips. The FE-SEM images demonstrated that the ZnO NWs were successfully grown in all sensor chips regardless of growth time. However, for short-term growth, the ZnO NWs were grown on the dendritic islands of the Au catalyst, as shown in Figure 3(A). No ZnO NWs grew on the Pt electrodes, heater, or

the bare silicon substrate in these synthesis conditions because of the catalytic activity of the discrete Au islands, which functioned as seeds for the ZnO NWs according to the VLS growth mechanism that was first reported in the work of Wagner and Ellis [27]. During heat treatment, the Au layer on the islands was partially melted to generate smaller dots of an average size of about 20 nm [28]. For the 10 min growth sample, the ZnO NWs were very short and could not come into contact with each other to form the NW-NW junctions. Thus, they could not constitute a proper conduction path of the electrical current for the sensor to operate. The roughly checked initial resistance of this sensor at room temperature was > 40 MΩ. Therefore, the gas-sensing test on this sample was omitted. However, the length of the ZnO NWs became longer when the growth time was increased to 60 min. For the 20 min growth sample, the ZnO NWs were long enough to come into contact with each other, and some NW-NW junctions were observed in the FE-SEM images (Figure 3(B)). However, the density of the ZnO NWs was still quite low; thus, the bare silicon substrate could be clearly seen between the Au catalyst islands. The sparse and fluffy structure of the sensing materials are very important because they enable the analytic gas molecules to come into contact with and adsorb on the surface of the NWs easily, thereby enhancing the sensitivity and accelerating the response/recovery time [29]. The length and the density of the ZnO NWs on the 40 min sample increased considerably, but the NWs were still isolated on the predefined Au catalyst islands from the surrounded Pt heater. In this sample, the ZnO NWs were long enough to make numerous NW-NW junctions, thereby bridging the two electrodes. The ZnO NW mat was also thicker; thus, the silicon substrate could hardly be seen (Figure 3(C)). When the growth time was further increased to 60 min, the ZnO NWs became even longer and many NWs grew out of the pre-defined Au catalyst islands and came into contact the with Pt heater (Figure 3(D)).
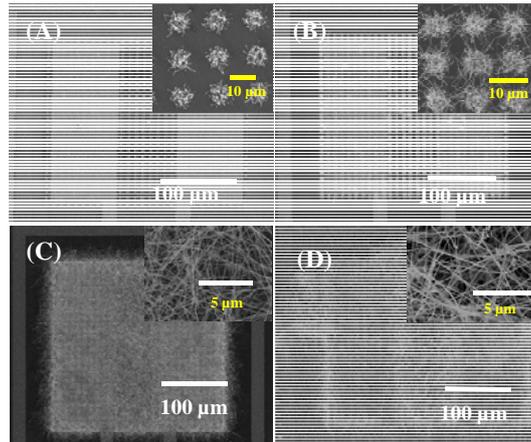
Figure 3. *SEM images of sensors fabricated at different growth times: (A) 10, (B) 20, (C) 40, and (D) 60 min. Insets are higher magnification images of corresponding samples*

The crystal structure of the synthesized NWs investigated via XRD is shown in Figure 4(A). The XRD pattern exhibits typical diffraction peaks at 2θ = 31.80°, 34.60°, 36.20°, 47.50°, 62.90°, and 67.90°, and these peaks correspond to the reflection of the (100), (002), (101), (102), (103), and (112) planes of the wurtzite hexagonal ZnO, respectively, with lattice constants of a = 0.325 nm and c = 0.521 nm (JCPDS, No. 36–1451). No characteristic diffraction peaks of the impurities corresponding to graphite and zinc carbide is observed in the XRD pattern, which indicates the successful growth of single phase ZnO NWs. Elemental analysis via EDS indicates the presence of C, O and Zn, where C is contamination and O and Zn originate from ZnO NWs (Figure 4(B)). The PL spectrum of ZnO NWs exhibits two emission peaks at ~380 (UV-band) and 520 nm (Green-band), as shown in Figure 4(C). The sharp UV peak originates from the combination of free excitations through an excitation-excitation collision process, which is also known as the near band-edge emission [30], whereas the Green-band is related to oxygen vacancy in ZnO as a result of structural defects [31]. The Green-band is very broad and asymmetrical because of the overlap of more than one peak, which indicates the existence of

different type of defects. The defect ratio defined by $\eta = I_{515}/I_{381}$ is relatively high, with $\eta \sim 5$, which indicates a high level of oxygen vacancies. This characteristic is an advantage for sensor application because a high level of oxygen vacancies indicates a high sensitivity to NO_2, as reported in [32]. The bandgap of ZnO NWs estimated from the PL measurement is 3.26 eV, which is smaller than that of the bulk form (3.7eV). According to the quantum confinement effect, the bandgap of ZnO NWs becomes larger than that of the bulk counterpart [33]. However, no quantum confinement effects were discovered in this study because the ZnO NWs have radii larger than 50 nm, whereas the bulk ZnO exciton Bohr radius is $\sim$2.34 nm [34].
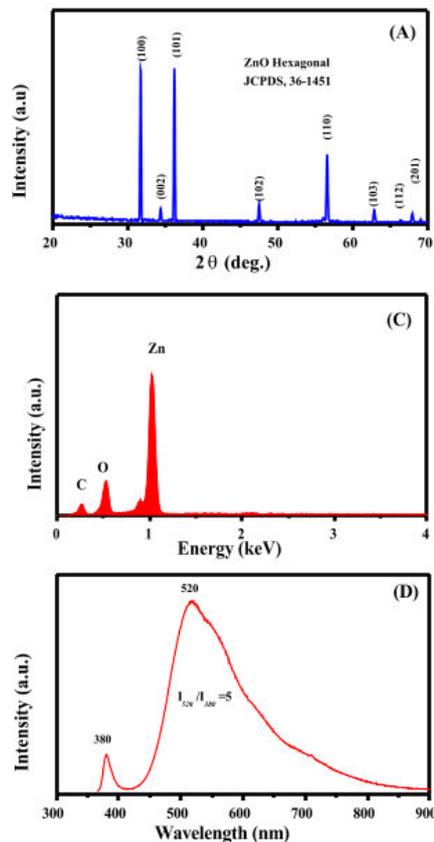

Figure 4. *Investigation of crystal structure and optical properties of the synthesized ZnO NWs via: (A) XRD pattern, (B) EDS analysis, and (C) PL spectrum*

Among common environmental polluting gases, NO_2 is one of the most toxic. Therefore, in this study, the gas sensing properties of the fabricated sensors for the detection of NO_2 were investigated. To investigate the effect of the length and density of ZnO NWs on the sensing performances, the response of the sensors to 0.5 ppm at 250 °C for three cycles was roughly checked, as seen in Figure 5. In all measured devices, the sensor resistance increased rapidly upon exposure to NO_2 because of the natural behavior of an n-type semiconductor [35]. The initial resistance measured at 250 °C was 235, 144, and 75 kΩ, whereas responsivity to 0.5 ppm NO_2 was 38%, 105%, and 49% for the sensors grown for 20, 40, and 60 min, respectively. The growth time significantly affected the length and density of the ZnO NWs, and consequently, the initial resistance and responsivity of the sensors. The growth time also affected the response and recovery characteristics of the sensors, i.e., the thicker NW mat required a longer time for gas molecules to diffuse into it and thus increased the response and recovery times of the devices. The response/recovery time (in seconds) were approximately 15/25 and 40/60 for the 20 and 60 min growth sensors, respectively.
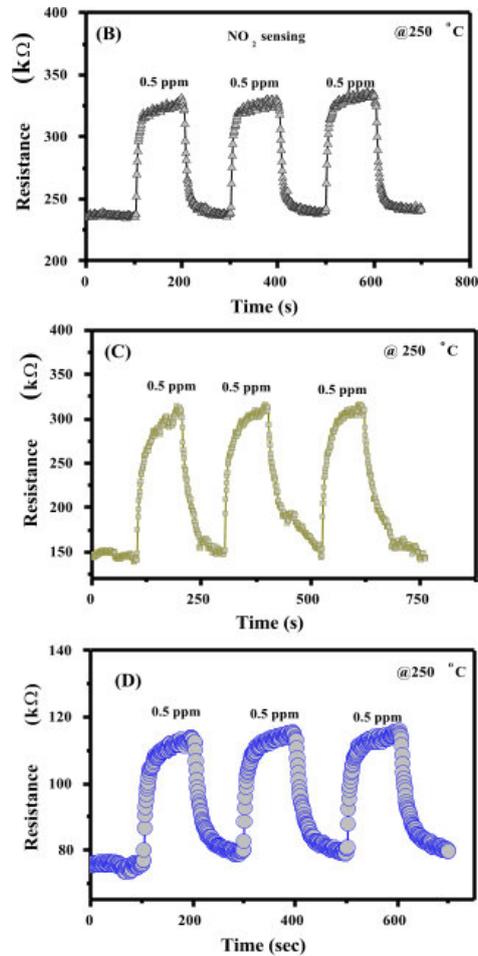
Figure 5. *Response to NO$_2$ of the sensors with ZnO NWs grown for (B) 20, (C) 40, and (D) 60 min.*

The gas sensitivity characteristics to NO$_2$, ethanol, and hydrogen were further investigated for the 40 min growth sensor, as seen in Figure 6. The sensor exhibited significant response to different concentrations of NO$_2$ at all measured temperatures ranging from 150 °C to 300 °C, as illustrated in Figure 6(A). The sensor response to 1 ppm NO$_2$ was 68%, 11%, 32%, and 51% at measured temperatures of 150 °C, 200 °C, 250 °C, and 300 °C, respectively. The highest response to NO$_2$ was observed at a temperature of 150 °C, followed by 300 °C, 250 °C, and 200 °C (Figure 6(B)). The temperature dependence of the NO$_2$ sensitivity to ZnO was determined via

the gas adsorption process, wherein the pre-adsorption of oxygen has an important function [36]. At a low temperature, that is, $\leq 150\ °C$, the NO_2 molecules were directly adsorbed on the surface of ZnO. At a high temperature, they were adsorbed on the surface of ZnO through the pre-adsorbed oxygen [37]. However, at a low working temperature of 150 °C, the sensor required significantly longer response and recovery times of about 200 and 350 sec, respectively. The response and recovery times decreased with increasing working temperature, and these values at 300 °C were about 15 and 20 sec, respectively. Figure 6(C-F) shows the transience resistance response to ethanol and hydrogen measured at temperature ranging from 300 °C to 450 °C. This behavior is inverse to the NO_2 sensing characteristics, specifically, the resistance of the sensor decreased upon exposure to reducing gases. Furthermore, the responsivity increased with increasing working temperature. The gas sensing characteristics at temperature higher than 450 °C were not measured because of the limitation of heaters on the devices. Regardless of the working temperature, the sensor required concentrations of analytic gas of 1 ppm NO_2, 250 ppm ethanol, or 100 ppm H_2 to obtain a responsivity of about 50%. This result indicated that the sensor showed a higher responsivity to NO_2 than to ethanol or hydrogen. However, only the sensor responses are presented because the stability and selectivity of the sensor are still being studied and will be reported elsewhere.
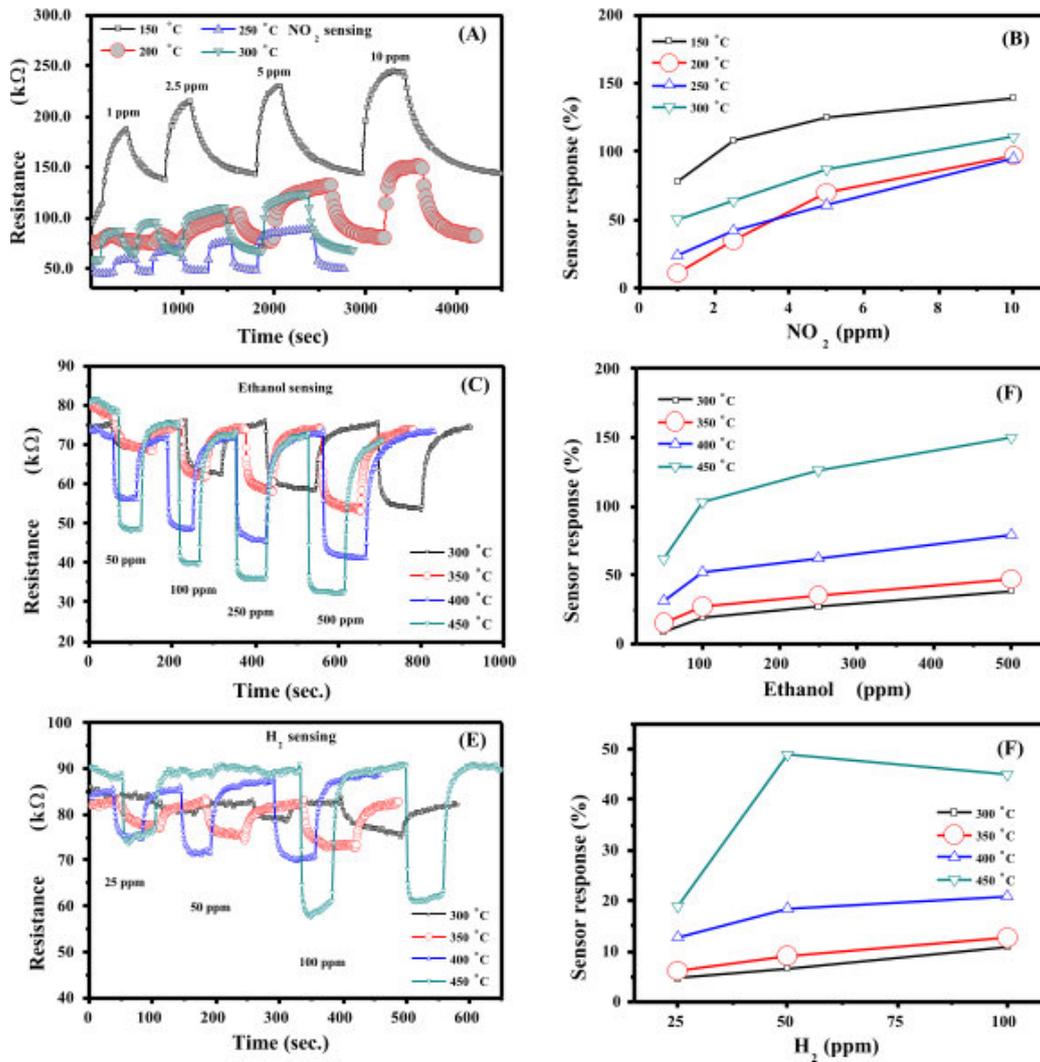
Figure 6. *Response to NO$_2$ (A,B), ethanol (C,D), and H$_2$ (E,F) of the ZnO NW-based sensor measured at different temperatures*

4. Conclusions

We introduced an effective design of a gas sensor based on ZnO NWs. The design was based on the use of dendrite catalytic Au islands for the growth of ZnO NWs via the CVD method. This design enabled the on-chip fabrication of a sensing material to create a precise predefined conduction path and to increase the number NW-NW junctions of the sensing material. The NWs

grown on the Au islands also eliminated the current leakage through the otherwise normally used seed layer. Gas sensing measurements indicated that the fabricated sensors are effective for the monitoring of NO_2 at a moderate temperature and can be used for the detection of ethanol and hydrogen at high temperatures.

Acknowledgements

References

[1]. N. D. Hoa, S. A. El-Safty, Meso- and Macroporous Co_3O_4 Nanorods for Effective VOC Gas Sensors, J. Phys. Chem. C, 115 (2011) 8466-8474

[2]. S. Tian, F. Yang, D. Zeng, C. Xie, Solution-Processed Gas Sensors Based on ZnO Nanorods Array with an Exposed (0001) Facet for Enhanced Gas-Sensing Properties, , J. Phys. Chem. C 116 (2012) 10586−10591

[3]. Zhihong Jing, Jinhua Zhan, Fabrication and Gas-Sensing Properties of Porous ZnO Nanoplates, Advanced Materials, 20 (2008) 4547–4551.

[4]. J. Huh, J. Park, G.T. Kim, J.Y. Park, Highly sensitive hydrogen detection of catalyst-free ZnO nanorod networks suspended by lithography-assisted growth, Nanotechnology, 22 (2011) 085502

[5]. M.K. Tsai, C.C.Huang, Y.C.Lee, C.S.Yang, H.C.Yu, J.W.Leec, S.Y.Hud, C.H.Chen, A study on morphology control and optical properties of ZnO nanorods synthesized by microwave heating, J. Luminescence, 132 (2012) 226–230.

[6]. M. Yin, M. Liu, S. Liu, Development of an alcohol sensor based on ZnO nanorods synthesized using a scalable solvothermal method, Sensors and Actuators B, 185 (2013) 735–742.

[7]. C.W. Na, H.S. Woo, I.D. Kim, J. H. Lee, Selective detection of NO_2 and C_2H_5OH using a Co_3O_4-decorated ZnO nanowire network sensor, Chemical Communications 47, (2011) 5148

[8]. S.D. Shinde, G.E. Patil, D.D. Kajale, V.B. Gaikwad, G.H. Jain, Synthesis of ZnO nanorods by spray pyrolysis for H_2S gas sensor, J. Alloys and Compounds, 528 (2012) 109–114

[9]. P. Hu, N. Han, D. Zhang, J. C. Ho, Y. Chen, Highly formaldehyde-sensitive, transition-metal doped ZnO nanorods prepared by plasma-enhanced chemical vapor deposition, Sensors and Actuators B: Chemical, 169 (2012) 74–80.

[10]. P. Rai, H.M. Song, Y.S. Kim, M.K. Song, P.R. Oh, J.M. Yoon, Y.T. Yu, Microwave assisted hydrothermal synthesis of single crystalline ZnO nanorods for gas sensor application, Materials Letters, 68 (2012) 90–93

[11]. J. D. Prades, R. Jimenez-Diaz, F. Hernandez-Ramirez, S. Barth, A. Cirera, A. Romano-Rodriguez, S. Mathur, and J. R. Morante, Ultralow power consumption gas sensors based on self-heated individual nanowires, Appl. Phys. Lett. 93, 123110 (2008)

[12]. K. D. Mitzner1, J. Sternhagen, D. W. Galipeau, Development of a micromachined hazardous gas sensor array, Sensors and Actuators B 93 (2003) 92–99

[13]. D.V. Dzung, K. Shibuya, T. T. Bui, S. Sugiyama, Micromachined NH_3 Gas Sensor with ppb-level Sensitivity Based on WO_3 Nanoparticles Thin film, Procedia Engineering, 25 (2011) 1149 – 1152

[14]. R. Calavia, A. Mozalev, R. Vazquez, I. Graciac, C. Cané, R. Ionescu, E. Llobet, Fabrication of WO_3 nanodot-based microsensors highly sensitive to hydrogen, Sensors and Actuators B, 149 (2010) 352–361

[15]. S. E. Moon, H.-K. Lee, N.-J. Choi, J. Lee, W. S. Yang, J. Kim, J.J. Jong, D.J. Yoo, Low-Power-Consumption Metal Oxide NO_2 Gas Sensor Based on Micro-Heater and Screen Printing Technology, Journal of Nanoscience and Nanotechnology, 12, (2012) 5543–5546(4)

[16]. H.J. Pandya, Sudhir Chandra, A.L. Vyas, Integration of ZnO nanostructures with MEMS for ethanol sensor Sensors and Actuators B 161 (2012) 923– 928

[17]. K. C. Chiang, Wan-Yu Wu, and Jyh-Ming Ting, Enhanced Lateral Growth of Zinc Oxide Nanowires on Sensor Chips, J. Am. Ceram. Soc., 94 [3] 713–716 (2011)

[18]. L. V. Thong, N. D. Hoa, D.T.T. Le, D.T. Viet, P. D. Tam, A. T. Le, N. V. Hieu, On-chip fabrication of SnO_2-nanowire gas sensor: The effect of growth time on sensor performance, Sensors and Actuators B, 146 (2010) 361–367.

[19]. M.-W. Ahn , K.-S. Park , J.-H. Heo, D.-W. Kim, K.J. Choi, J.-G. Park, On-chip fabrication of ZnO-nanowire gas sensor with high gas sensitivity, Sensors and Actuators B, 138 (2009) 168–173.

[20]. L. Guo, H. Zhang, D. Zhao, B. Li, Z. Zhang, M. Jiang, D. Shen, High responsivity ZnO nanowires based UV detector fabricated by the dielectrophoresis method, Sensors and Actuators B 166– 167 (2012) 12–16

[21]. L. Vayssieres, Growth of arrayed nanorods and nanowires of ZnO from aqueous solution, Advanced Materials, 15 (2003) 464–466

[22]. L. E. Greene, M. Law, D. H. Tan, M. Montano, J. Goldberger, G. Somorjai, P. Yang, General Route to Vertical ZnO Nanowire Arrays Using Textured ZnO Seeds, Nano Letters 5 (7), pp 1231–1236

[23]. N. V. Hieu, N. D. Chien, Low-temperature growth and ethanol-sensing characteristics of quasi-one-dimensional ZnO nanostructures, Physica B: Condensed Matter, 403 (2008) 50–56.

[24]. N. D. Khoang, H. S. Hong, D. D. Trung, N. V. Duy, N. D. Hoa, D. D. Thinh, N. V. Hieu, On-chip growth of wafer-scale planar-type ZnO nanorods sensors for effective detection of CO gas, Sensors and Actuators B, 181 (2013) 529–536

[25]. J. Wang, J. Sha, Q. Yang, X. Ma, H. Zhang, J. Yu, D. Yang, Carbon-assisted synthesis of aligned ZnO nanowires, Materials Letters, 59 (2005) 2710–2714

[26]. Z. Ankara, T. Kammerer, A. Gramm, A. Schütze, Low power virtual sensor array based on a micromachined gas sensor for fast discrimination between H_2, CO and relative humidity, Sensors and Actuators B 100 (2004) 240–245

[27]. R.S. Wagner and W.C. Ellis, Vapor-Liquid-Solid mechanism of single crystal growth, Appl. Phys. Lett. 4 (1964) 89–90

[28]. D. D. Trung, N. V. Toan, P. V. Tong, N. V. Duy, N. D. Hoa, N. V. Hieu, Synthesis of single-crystal SnO_2 nanowires for NO_x gas sensors application, Ceramics International, 38 (2012) 6557–6563

[29]. N. D. Hoa, N. V. Quy, Y. Cho, D. Kim, Porous single-wall carbon nanotube films formed by in Situ arc-discharge deposition for gas sensors application, Sensors and Actuators B, 135 (2009) 656–663

[30]. D. C. Reynolds, D. C. Look, B. Jogai, C. W. Litton, T. C. Collins, W. Harsch, G. Cantwell, Neutral-donor-bound-exciton complexes in ZnO crystals, Phys. Rev. B57 (1998) 12151–12155

[31]. O. D. Jayakumar, V. Sudarsan. C. Sudakar, R. Naik, R. K. Vatsa, A. K. Tyagi, Green emission from ZnO nanorods: a role of defects and morphology, Scripta. Mater. 62 (2010) 662–665

[32]. M.-W. Ahn, K.-S. Park, J.-H. Heo, J.-G. Park, D.-W. Kim, K. J. Choi, J.-H. Lee, and S.-H. Hong, Gas sensing properties of defect-controlled ZnO-nanowire gas sensor, Appl. Phys. Lett. 93 (2008) 263103

[33]. Quantum confinement in ZnO nanorods, Appl. Phys. Lett. 85 (2004) 3833

[34]. R. T. Senger and K. K. Bajaj, Optical properties of confined polaronic excitons in spherical ionic quantum dots, Phys. Rev. B, 68 (2003) 045313

[35]. H. V. Han, N. D. Hoa, P. V. Tong, H. Nguyen, N. V. Hieu, Single-crystal zinc oxide nanorods with nanovoids as highly sensitive NO_2 nanosensors, Materials Letters, 94 (2013) 41–43

[36]. M. Chen, Z. Wang, D. Han, F. Gu, G. Guo, High-sensitivity NO_2 gas sensors based on flower-like and tube-like ZnO nanomaterials, Sensors and Actuators B, 157 (2011) 565–574

[37]. B. Shouli, C. Liangyuan, H. Jingwei, L. Dianqing, L. Ruixian, C. Aifan, C.C. Liu, Synthesis of quantum size ZnO crystals and their gas sensing properties for NO_2, Sensors and Actuators B, 159, (2011) 97–102

<Research highlights>

►Gas sensors based on the length and density of controlled ZnO nanowires were obtained by growing the nanowires on discrete islands of an Au catalyst ►The design increased the nanowire-nanowire junctions and eliminated current leakage through the normally used seed layer ►These sensors can be used in the monitoring of NO_2, H_2, and/or ethanol by choosing the working temperature.

<**Biography of the authors**>

Hugo Nguyen received the M.Sc. degree in machine engineering in 1992 and PhD degree in microsystem technology in 2006, both in Sweden. He has been working in The Ångström Space Technology Centre at Uppsala University since 2000 and has a special interest in all kinds microsystems for both space and non-space applications. Since 2007, he has been working on magnetic field sensors made of AMR, TMR materials, and chemical sensors including gas sensors using nanomaterials of metal oxides, and microfluidic systems.

Chu Thi Quy obtained her bachelor degree in Engineering of Education at Hanoi Pegadogical University No. 2, Vietnam in 2011. Currently, she is a master student in solid state physic at the same university, but doing research for graduation thesis at International Training Institute for Material Science (ITIMS), Hanoi University of Science and Technology (HUST). Her research focuses on the synthesis and functionalization of zinc oxide nanowires for gas sensing application.

Nguyen Duc Hoa obtained his PhD degree in material science and engineering in 2009 at Chungnam National University in Korea. He awarded JSPS fellowship and conducted the research at National Institute for Material Science (NIMS, Japan) from 2009 to 2011. His research activities cover a wide range of nanostructured materials from synthesis, fundamental study, and applications. Currently, he holds the position as a lecturer and scientist at Hanoi University of Science and Technology, Vietnam.

Nguyen The Lam received his MSc. degree in Material Science from International Training Institute for Material Science in 1997 and Ph.D. degree in Solid State Physics from Hanoi University of Science and Technology in 2005. Currently, he is lecturer and researcher at Faculty of Physics, Hanoi Pedagogical University No.2 Vietnam. His research interests include nanomaterials and their simulations.

Nguyen Van Duy is currently working as a lecturer and researcher at International Training Institute for Material Science (ITIMS), Hanoi University of Science and Technology (HUST).

He received his PhD degree from the Department of Electrical and Electronics Engineering at Sungkyunkwan University, South Korea, in 2011. His current research interests include nanomaterials, nanofabrications, characterizations, and applications to electronic devices, gas sensors, and biosensors.

Vu Van Quang joined the International Institute for Material Sciences (ITIMS) at Hanoi University of Science and Technology (HUST) as a researcher and lecturer in 2010. He received his Master degree from University of Paris 11, France in 2005, and PhD degree from University of Wales, Aberystwyth, United Kingdom in 2008. Then he moved to Max-Planck Institute for Metals Research, Stuttgart, Germany to do his post-doctoral work until Jun 2010. His current research interests include synthesis and application of graphene for electronic devices, gas sensors and biosensors.

Nguyen Van Hieu joined the International Training Institute for Material Science (ITIMS) at Hanoi University of Science and Technology (HUST) in 2004, where he currently is an Associate Professor. He received his PhD degree from the Faculty of Electrical Engineering at University of Twente in The Netherlands in 2004. He worked as a post-doctoral fellow at the Korea University from 2006-2007. His current research interests include functional nanostructures, gas sensors, and biosensors.